JOURNAL OF SOLID STATE CHEMISTRY 116, 15–27 (1995)

Phase Composition, Microstructure, and Sintering in the System Co–Li_2CO_3

A. Marini, V. Berbenni, V. Massarotti, and D. Capsoni

Dipartimento di Chimica Fisica, Università di Pavia, Viale Taramelli 16, 27100 Pavia, Italy

and

E. Antolini

Ansaldo Ricerche Srl, Corso Perrone 25, 16161 Genoa, Italy

Received February 7, 1994; in revised form July 25, 1994; accepted July 28, 1994

Co and Li_2CO_3 were used as starting materials to obtain cobalt-based plaques of potential use in molten carbonate fuel cell technology. Samples were prepared by thermal treatments in the temperature range 800–1300°C. Their composition and microstructure have been investigated at room temperature by X-ray diffraction analysis (Rietveld refinement), weight change and density data, porosimetry, and scanning electron microscopy. It is shown that a highly nonstoichiometric Co_3O_4 forms on lithium-containing samples in the entire temperature range investigated, while a stoichiometric Co_3O_4 is always obtained in the absence of Li. Moreover, clear evidence has been obtained that sinterization starts at lower temperatures on lithiated samples than on pure Co ones and that it causes the formation of consistent amounts of stoichiometric CoO in both types of sample. It is argued that the increased sinterization rate shown by Li-containing samples is due to the highly defective structure of their Co_3O_4 phase.

1. INTRODUCTION

In molten carbonate fuel cell (MCFC) technology, the dissolution of the state of the art, lithiated NiO cathode in the electrolyte is one of the major cell lifetime limiting factors (1). To overcome this problem, research is carried out on alternative cathode materials suitable to replace NiO (2, 3). In this respect cobalt-based materials, particularly $LiCoO_2$, seem to be promising candidates because of their low dissolution rate in molten carbonates (4, 5). However, as is well known, cathodic materials for MCFC are not merely electronic conductors, but must show relevant catalytic properties. As a consequence, cathode performances are affected not only by the nature, but also by the microstructure of the cathode (6). The result is that control of the microstructure is often the difficult step in cathode preparation. With this in mind we approached the study of cobalt-based materials for MCFC by selecting, as the starting system, the solid state system Co–Li_2CO_3. Such a selection was suggestd by our previous studies on the system Ni–Li_2CO_3 which showed that some degree of microstructural control of the lithiated NiO cathodes was possible, due to the presence of lithium carbonate (7, 8). Our final aim is to fully understand the reactive processes taking place in the system Co–Li_2CO_3 and to characterize both from a structural and microstructural point of view the different phases that can be obtained from such a system. A detailed analysis of the reactive processes is actually underway and will be soon published. In this paper attention will be focused on the phase composition and sintering behavior of manufacts (plaques) obtained by different thermal treatments.

2. EXPERIMENTAL

2.1. Products

Cobalt (Matthey, 99.8%, 1.6 μm) and lithium carbonate (Merck 5671) have been used as starting materials. Mixtures of these powders (composition $x_{Li} = 0.00, 0.10, 0.20$ with x_{Li} = lithium cationic fraction) were ball milled for 24 hr in a polyethylene container together with a binder (Methocel MC Fluka Chemie 64620, 400 mPa), an antifoaming agent (Dow Corning antifoam A compound), and deionized water (the mass ratio cobalt/organic substances was 12.5/1 in each sample). The resulting slurries were degassed and then cast onto beeswax-coated glass surfaces with a blade thickness of 2 mm at a shear rate of 2 cm/min. After the tapes were sufficiently dried, disk samples (diameter of 3 cm) were finally cut from them.

0022-4596/95 $6.00

The thickness of the samples so obtained was about 0.5 mm. The sample plaques were then put on porous alumina platforms and subjected to the following thermal cycle: (a) heating (2.0°C/min) from room temperature to temperatures in the range 800–1300°C; (b) isotherm of 5 hr at the maximum temperature; (c) cooling (2.0°C/min) to room temperature. Thermal treatments were performed in air by a BICASA BE 35 furnace. Plaque diameter was measured before and after thermal treatment by a precision gauge.

2.2. Apparatus and Procedures

2.2.1. Porosimetric measurements. Samples porosity was measured by a Micromeritics Instrument Corp. Autopore II 9220 scanning mercury porosimeter.

2.2.2. Density measurements. Sample densities were determined by a picnometric method using Hg as a fluid and the dilatometer of the porosimeter as a picnometer. The density is obtained with this method by mass measurements of (a) the sample, (b) the dilatometer filled with Hg, and (c) the dilatometer containing the sample and filled with Hg up to the same level as in (b). When the three mass values are known, the volume of the sample, and then its density, can easily be calculated.

2.2.3. Diffractometric measurements. Diffraction data were obtained by a Philips PW 1710 powder diffractometer equipped with a Philips PW 1050 vertical goniometer and with a graphite bent crystal monochromator. Use was made of both Cu$K\alpha$ ($K\alpha_1$ = 1.5406 Å; $K\alpha_2$ = 1.5443 Å) and Fe$K\alpha$ radiation ($K\alpha_1$ = 1.9360 Å; $K\alpha_2$ = 1.9399 Å). Data were collected in step-scan mode with a step width of 0.03° and counting time of 1 sec in the angular ranges $15° < 2\theta < 145°$ (Cu$K\alpha$) and $20° < 2\theta < 150°$ (Fe$K\alpha$). Structural data concerning the different phases and their relative amounts were obtained according to the Rietveld refinement method (9). The refinement of the structural and profile parameters was performed with the program DBW3-2S (10). Regarding the refinement procedure, some change was introduced with respect to the procedure previously described (11): (a) variation of oxygen coordinates in both the Co_3O_4 [x(O)] and $LiCoO_2$ [z(O)] phases. Such a variation was introduced in the isotropic thermal parameter optimization step (step 5 of Ref. 11); (b) variation of site occupancies in Co_3O_4 which was added immediately after the refinement of thermal parameters; (c) introduction of a preferred orientation parameter, according to the March–Dollase equation (12), for the CoO phase of lithium-containing samples. This step was added before the refinement of asymmetry and profile width parameters (step 4 of Ref. 11). The density of each phase was obtained from the pertinent cell volume and mass which were in turn obtained from the refined parameters. The mass fractions of the different phases were calculated according to the procedure of Hill and Howard (13).

Both the refined parameters and the mass fractions were substantially independent of the radiation utilized.

2.2.4. Microscopic measurements. SEM micrographs were collected with a Cambridge Stereoscan 200 scanning electron microscope.

3. RESULTS

3.1. Mass Changes

Table 1 summarizes the percentage mass changes at room temperature by mixtures of different composition subjected to different thermal treatments. As can be seen there are threshold temperature values beyond which the weight changes decrease with increasing temperature. Such threshold values can be roughly put at $T \approx 1100$°C for lithium-containing samples and $T \approx 1200$°C for pure Co samples.

3.2. X-Ray Measurements

X-ray diffraction patterns of pure Co samples treated in the temperature range 800–1200°C are shown in Fig. 1. As can be seen, Co_3O_4 is the only phase present for temperatures up to 1100°C while for higher temperatures there is evidence of CoO also. Figure 2 shows the diffraction patterns of the $x_{Li} = 0.10$ samples in the same temperature range as in Fig. 1. Now there are two phases up to 1000°C: Co_3O_4 and $LiCoO_2$. For $T = 1100$°C CoO begins to appear and its presence becomes evident for $T > 1100$°C. However the reflections of this new phase are

TABLE 1

Mass Changes (%) Measured at Room Temperature on Plaques of Different Initial Composition and Subjected to Different Thermal Treatments

	Composition (x_{Li})[a]		
Temperature (°C)	0.00	0.10	0.20
800	26.1	18.1	13.8
900	26.1	18.1	13.7
1100	26.1	17.5	12.5
1200	25.7	15.3	9.3
1300	23.7	10.9	4.5
Expected	26.11	21.37	15.98

Note. The temperature reported is the highest reached in the pertinent thermal cycle.

The expected values have been calculated on the basis of the formation of pure Co_3O_4 ($x_{Li} = 0.00$) or stoichiometric amounts of Co_3O_4 and $LiCoO_2$ ($x_{Li} > 0.00$).

[a] X_{Li} is the lithium cationic fraction.

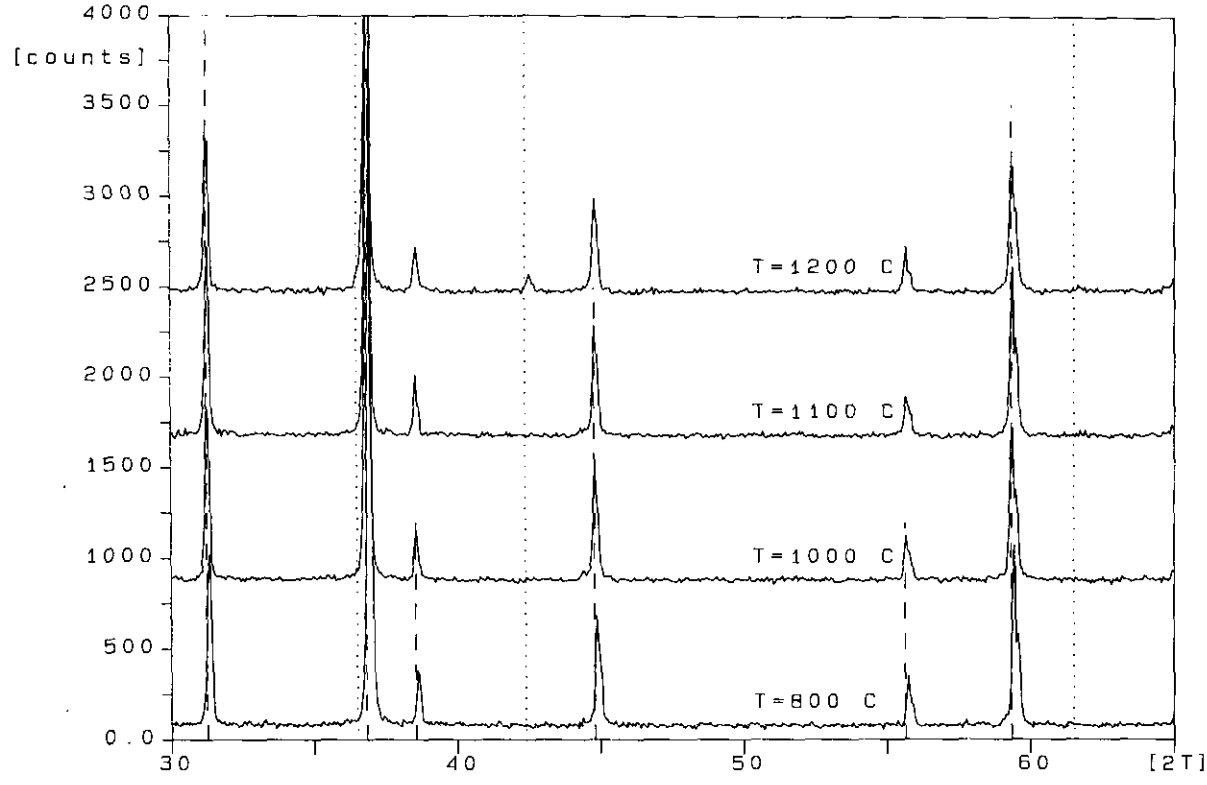

FIG. 1. X-ray diffraction patterns of pure Co plaques after different thermal treatments. Reference angular positions: Co_3O_4 (dashes); CoO (points). A vertical shift of 800 counts between two adjacent patterns must be considered.

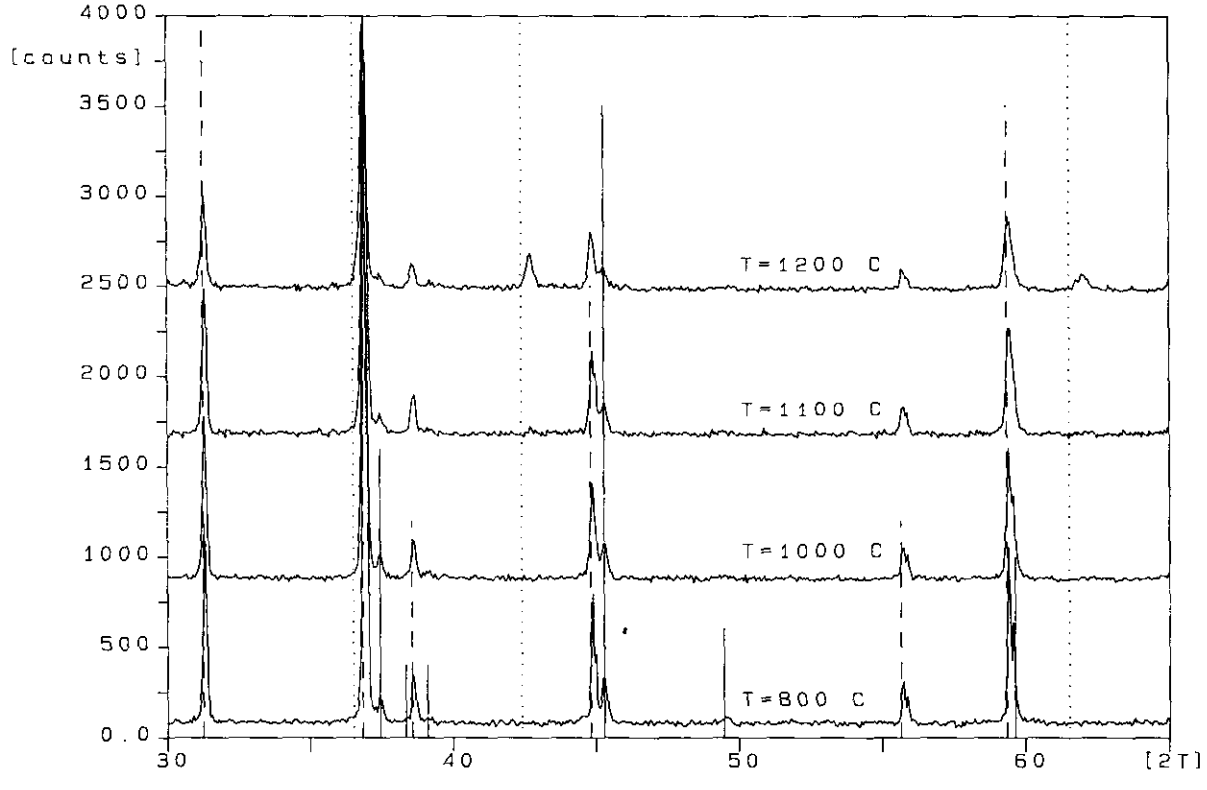

FIG. 2. X-ray diffraction patterns of $x_{Li} = 0.10$ plaques after thermal treatments at different temperatures. Reference angular positions: Co_3O_4 (dashes); CoO (points); $LiCoO_2$ (line). A vertical shift of 800 counts between two adjacent patterns must be considered.

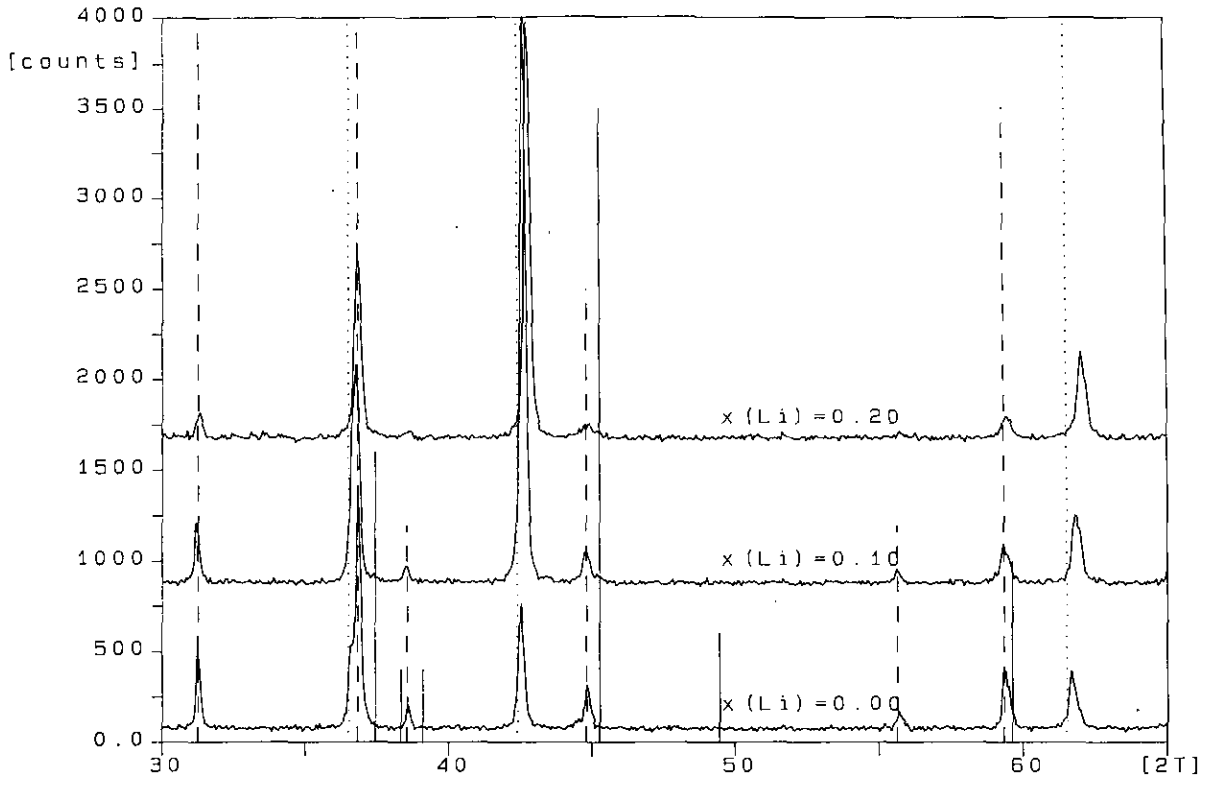

FIG. 3. X-ray diffraction patterns of pure Co and lithium-containing plaques after thermal treatments at 1300°C. Reference angular positions: Co_3O_4 (dashes); CoO (points); $LiCoO_2$ (line). A vertical shift of 800 counts between two adjacent patterns must be considered.

shifted toward angles slightly higher than expected. Samples of nominal composition $x_{Li} = 0.20$ show the same behavior, the only difference being that the CoO reflections are even more shifted toward higher angles (see Fig. 3). It is likely that such a shift is almost in part due to the substitution of a few Li atoms for Co atoms in the CoO lattice with the formation of a solid solution of the type $Li_xCo_{1-x}O$. However, the shift toward higher angles is not the only feature of the CoO phase of lithium-containing samples. It can be seen in Fig. 3 that the intensity ratio between the reflections at $2\theta = 42.4°$ and $2\theta = 61.5°$ (both these reflections are due to CoO only) is much higher than the expected value of 2 for both lithium-containing samples. The nature of the phases present in the different samples at each temperature is summarized in Table 2.

3.3. Plaque Diameter Measurements

The difference between the plaque diameter change (following thermal treatment) measured on pure Co and $x_{Li} = 0.10$ samples is shown as a function of the temperature of the thermal treatment in Fig. 4. As can be seen, such a difference reaches a maximum at about 1100°C.

3.4. Density and Porosity Measurements

The ratio of actual density/theoretical density (hereafter referred to as relative density) after thermal treatment

TABLE 2

Phase Composition (as Deduced by X-Ray Analysis) of Pure Co and Lithium-Containing Plaques after Thermal Treatment at Different Temperatures

	Composition (x_{Li})		
Temperature (°C)	*0.00*	*0.10*	*0.20*
800	Co_3O_4	Co_3O_4 $LiCoO_2$	Co_3O_4 $LiCoO_2$
1000	Co_3O_4	Co_3O_4 $LiCoO_2$	Co_3O_4 $LiCoO_2$
1100	Co_3O_4	Co_3O_4 $LiCoO_2$ CoO	Co_3O_4 $LiCoO_2$ CoO
1200	Co_3O_4 CoO	Co_3O_4 $LiCoO_2$ CoO	Co_3O_4 $LiCoO_2$ CoO
1300	Co_3O_4 CoO	Co_3O_4 CoO	Co_3O_4 $LiCoO_2$ CoO

at 800°C is reported for pure Co and $x_{Li} = 0.10$ samples in Table 3. As the lithium-containing sample was biphasic, its theoretical density has been obtained by taking into account the relative amount of each phase with the relationship

$$d_{th} = \frac{d_{th,L}\, d_{th,C}}{\sigma_L d_{th,C} + (1 - \sigma_L) d_{th,L}} \quad [1]$$

where $d_{th,L}$ is the theoretical density of $LiCoO_2$; $d_{th,C}$ is the theoretical density of Co_3O_4; and σ_L is the mass fraction of $LiCoO_2$ in the sample.

The σ_L values have been obtained under the assumption that all the lithium originally in the sample was transformed into $LiCoO_2$. The theoretical densities of Co_3O_4 (cubic) and $LiCoO_2$ (hexagonal) were calculated from the lattice constants obtained by X-ray measurements:

Co_3O_4: $a = 8.0834$ Å, $d = 6.06$ g/cm^3;
$LiCoO_2$: $a = 2.8156$ Å, $c = 14.0719$ Å, $d = 5.12$ g/cm^3.

In both cases the values obtained are in good agreement with those of the literature (14, 15).

Porosity data concerning pure Co and $x_{Li} = 0.10$ samples are also reported in Table 3. Total porosity has been calculated using the relationship (16)

$$P = 1 - \frac{d}{d_{th}}, \quad [2]$$

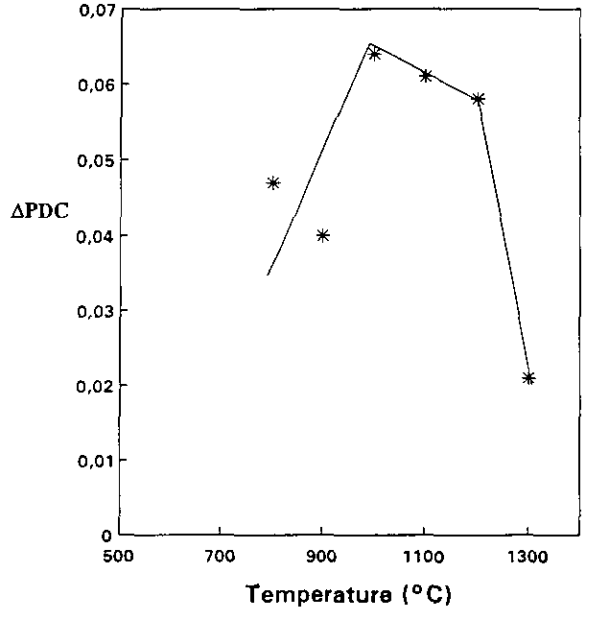

FIG. 4. ΔPDC as a function on the temperature. ΔPDC represents the difference between the plaque diameter change shown by pure Co and $x_{Li} = 0.10$ plaques after thermal treatment.

TABLE 3
Density and Porosity Data for Pure Co and Lithium-Containing Plaques after Thermal Treatments at Different Temperatures

	$x_{Li} = 0.00$°C		$x_{Li} = 0.10$	
	$T = 800$°C	$T = 1200$°C	$T = 800$°C	$T = 1200$°C
Hg porosity (%) (macro + meso)	65	43	64	44
Relative density	0.33		0.29	
Total porosity (%) from Eq. (2)	67		71	
Microporosity (%)	2		7	
MPS (μm) (macro + meso)	0.4	1.6	0.2	0.3

Note. The lower limit of the mesopores diameter is 0.003 μm. Micropores are still smaller (see text for details on their determination).

where d represents the experimental density. As shown in Table 3, Hg porosity (macropores + mesopores) depends on temperature but is independent of sample composition. Total porosity, on the contrary, is slightly higher for the lithium-containing sample. The mean pore size (macropores + mesopores) values for pure Co samples are two times greater ($T = 800$°C) or more than five times greater ($T = 1200$°C) than those of the lithium-containing samples.

3.5. Scanning Electron Microscopy

Micrographs of pure Co and lithium-containing samples after thermal treatments at 800, 1000, 1100, 1200, and 1300°C are shown in Figs. 5, 6, and 7. Both the magnification and the scale are reported in each micrograph (top left). As can be seen, they are very similar for all the micrographs so that grain sizes can be directly compared. It is apparent that there is considerable grain growth with increasing temperature and that such growth starts at a lower temperature on lithium-containing samples.

4. DISCUSSION

4.1. Mass Change Data and Co_3O_4 Stoichiometry

To discuss the mass change data of Table 1 some information is necessary, from our study on powders, about the reactive processes occurring in the system:

(a) the first product of Co oxidation, in air, is Co_3O_4;

(b) at temperatures around 930°C, Co_3O_4 completely transforms into CoO. Such a reaction is a reversible one and, provided that the cooling rate is low enough (as in the present work) it takes place quantitatively during the cooling of samples (in air);

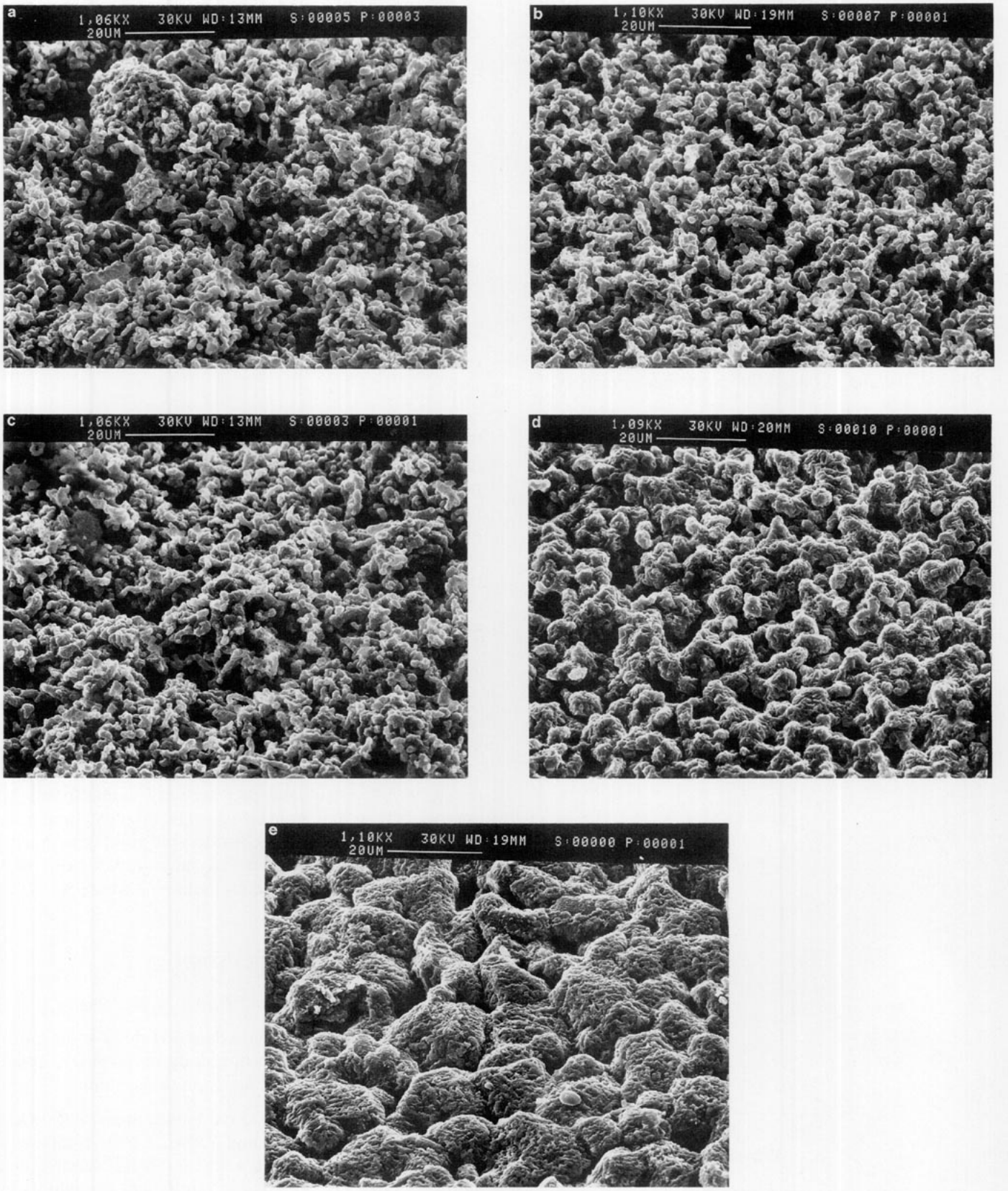

FIG. 5. Micrographs of pure Co plaques after thermal treatments at different temperatures: (a) 800°C; (b) 1000°C; (c) 1100°C; (d) 1200°C; (e) 1300°C.

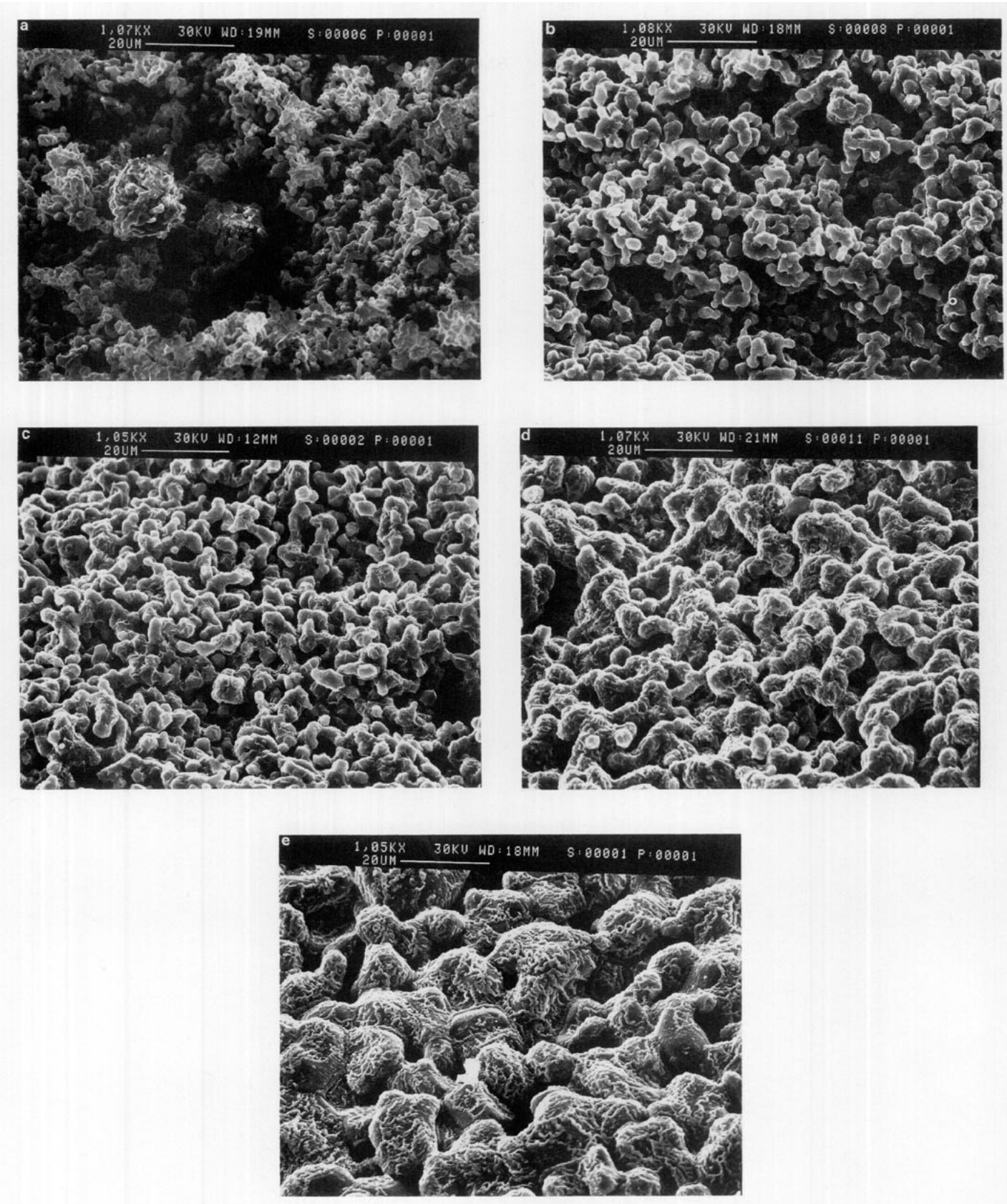

FIG. 6. Micrographs of $x_{Li} \approx 0.10$ plaques after thermal treatments at different temperatures: (a) 800°C; (b) 1000°C; (c) 1100°C; (d) 1200°C; (e) 1300°C.

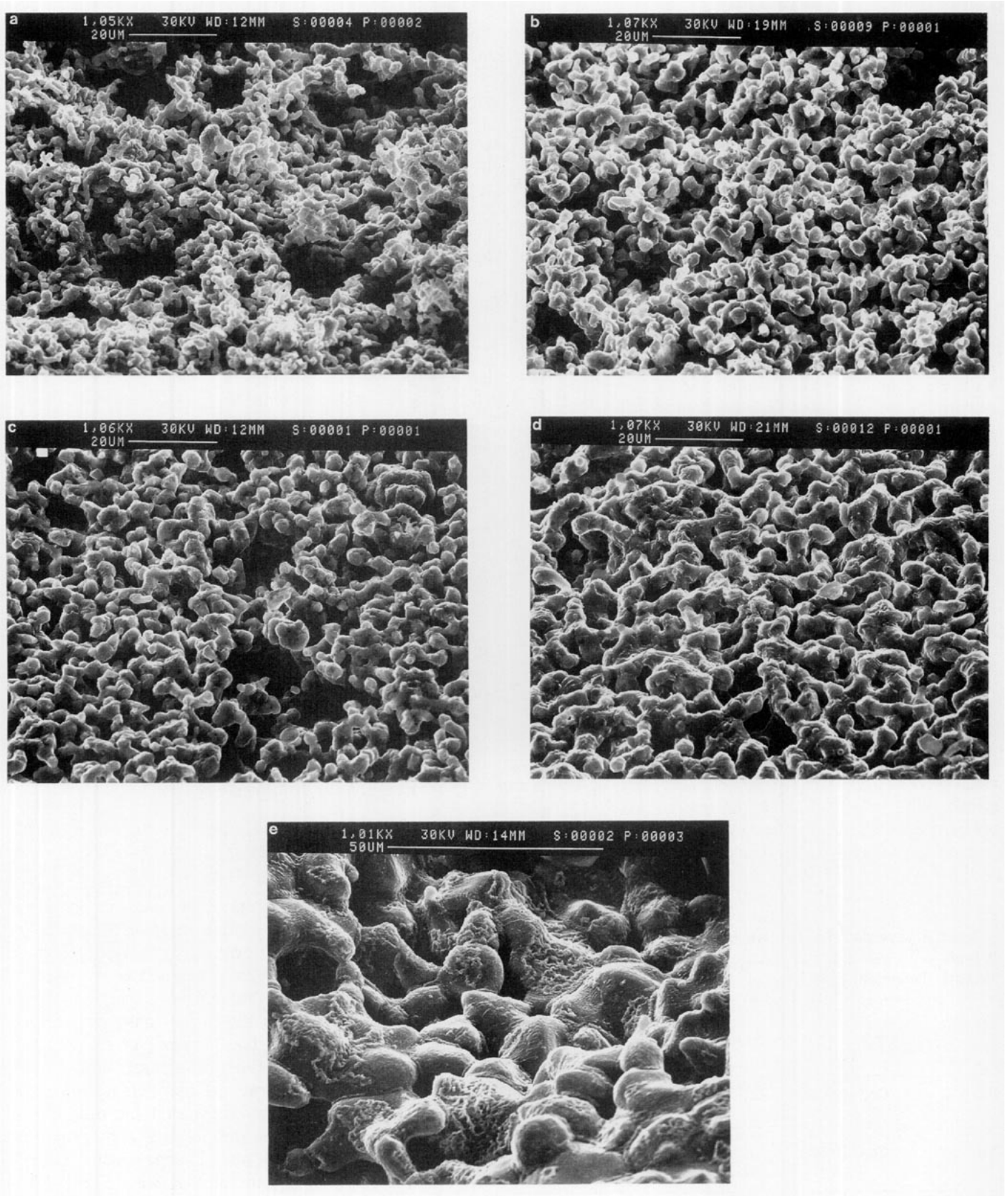

FIG. 7. Micrographs of $x_{Li} = 0.20$ plaques after thermal treatments at different temperatures: (a) 800°C; (b) 1000°C; (c) 1100°C; (d) 1200°C; (e) 1300°C.

(c) in both $x_{Li} = 0.10$ and $x_{Li} = 0.20$ mixtures, the Li_2CO_3 quantitatively transforms into $LiCoO_2$ during Co oxidation and well before $Co_3O_4 \rightarrow CoO$ transformation;

(d) lithium loss from pure $LiCoO_2$ becomes apparent at $T \geq 1100°C$.

Point (d) could be responsible for lower than expected mass changes. However, no problem should exist for samples obtained at $T < 1100°C$. As expected and as confirmed by X-ray data (see Table 2) they contain only Co_3O_4 ($x_{Li} = 0.00$) or $Co_3O_4 + LiCoO_2$ ($x_{Li} = 0.10; 0.20$) and their expected mass changes can be easily calculated by considering the pertinent net reaction (and complete organic substances burnout). The results are reported in the last row of Table 1. As can be seen the mass change recorded for the pure Co sample at $T < 1100°C$ agrees with the expected value, while those measured on lithium-containing samples are appreciably lower than the calculated ones. A good hypothesis to explain the observed differences is that a stoichiometric Co_3O_4 is obtained from pure Co samples while a highly nonstoichiometric oxide forms in the lithiated samples. Both the stoichiometry and the relative amount of the Co_3O_4 can then be easily calculated from experimental mass change data.

The results obtained for $T = 800°C$ are given in Table 4. Obviously gravimetric data alone cannot prove the hypothesis and independent measurements are necessary to determine the Co_3O_4 stoichiometry.

4.2. X-Ray Data and Co_3O_4 Stoichiometry

X-ray data have been refined to find the stoichiometry and the relative amounts of the different phases obtained after thermal treatment at $T < 1100°C$. The results obtained for $T = 800°C$ are given in Table 4 and can be compared at a glance with the gravimetric ones. It appears that X-ray data fully confirm both the stoichiometric nature of the Co_3O_4 phase obtained from pure Co plaques and the nonstoichiometric nature of the oxide phase obtained from lithiated samples. A brief discussion is, however, necessary regarding the quantitative agreement between X-ray and mass change data. As can be seen in Table 4, higher $LiCoO_2$ amounts are obtained from the first ones. However, both nonstoichiometry and relative amounts of the two phases have been obtained by gravimetric data, on the assumption that the entire lithium content of the original mixture transforms into $LiCoO_2$. This simply means that mass percentages of $LiCoO_2$ higher than those obtained by weight change data are impossible and that, as a consequence, X-ray data overestimate the relative amount of the $LiCoO_2$ phase. To understand why, the experimental and calculated patterns of the $x_{Li} = 0.20$ sample are compared, as an example, in Fig. 8. As can be seen, the agreement is very good, suggesting that the error source is in the scale factor (by which the relative amounts of the different phases are determined) rather than in the crystallographic model. Such an error source depends after all on microabsorption, the effect of which, as is well known in the literature (17–21), is to underestimate the contribution of the phase with the higher absorption coefficient for the X-ray radiation utilized (Co_3O_4 in our case; obviously if Co_3O_4 is underestimated, $LiCoO_2$ is overestimated).

The percentages given in square brackets in Table 4 are related to $LiCoO_2$ and have been obtained on the basis of the recorded mass change and under the assumption that the stoichiometry of the cobalt oxide is that deduced from X-ray data. As can be seen, they are very similar to those deduced from gravimetric data, confirming that the lower than expected mass changes obtained for these samples are only due to oxygen defect.

TABLE 4

Stoichiometry and Relative Amounts of the Different Phases Present on Pure Co and Lithium-Containing Plaques after Thermal Treatment at 800°C

	x_{Li}		
	0.00	0.10	0.20
X-ray	Co_3O_4(100%)	$LiCoO_2$(19.0%) [13.4%]	$LiCoO_2$(33.2%) [30.0%]
		$Co_3O_{3.82}$(81.0%)	$Co_3O_{3.64}$(66.8%)
Δm	Co_3O_4(100%)	$LiCoO_2$(13.7%)	$LiCoO_2$(30.0%)
		$Co_3O_{3.54}$(86.3%)	$Co_3O_{3.60}$(70.0%)

Note. The percentages reported in square brackets are those expected for the $LiCoO_2$ phase on the basis of the recorded mass change and of the stoichiometry deduced from X-ray data (see text).

4.3. Phase Composition and Temperature: Pure Co Samples

It can be seen in Table 1 that the mass change measured in pure Co mixtures after thermal treatment at 1300°C is about 2.4 units lower than that recorded at 800°C. Table 2 shows that CoO is now present together with Co_3O_4. As the X-ray refinement shows that both phases are stoichiometric, the entire mass change decrease must be explained on the basis of the relative amount of the CoO phase. The mass percentages of the two oxides obtained by X-ray and mass change data are reported in Table 5. It may seem that the differences between the results are quite high, however, as $M(Co_3O_4)/3M(CoO) = 1.07$, mass change is not very sensitive to the relative amount of the two oxides. As a consequence the Δm value expected on the basis of the X-ray composition is only 3.5% lower than the measured one. Moreover, if reference is made to the total plaque

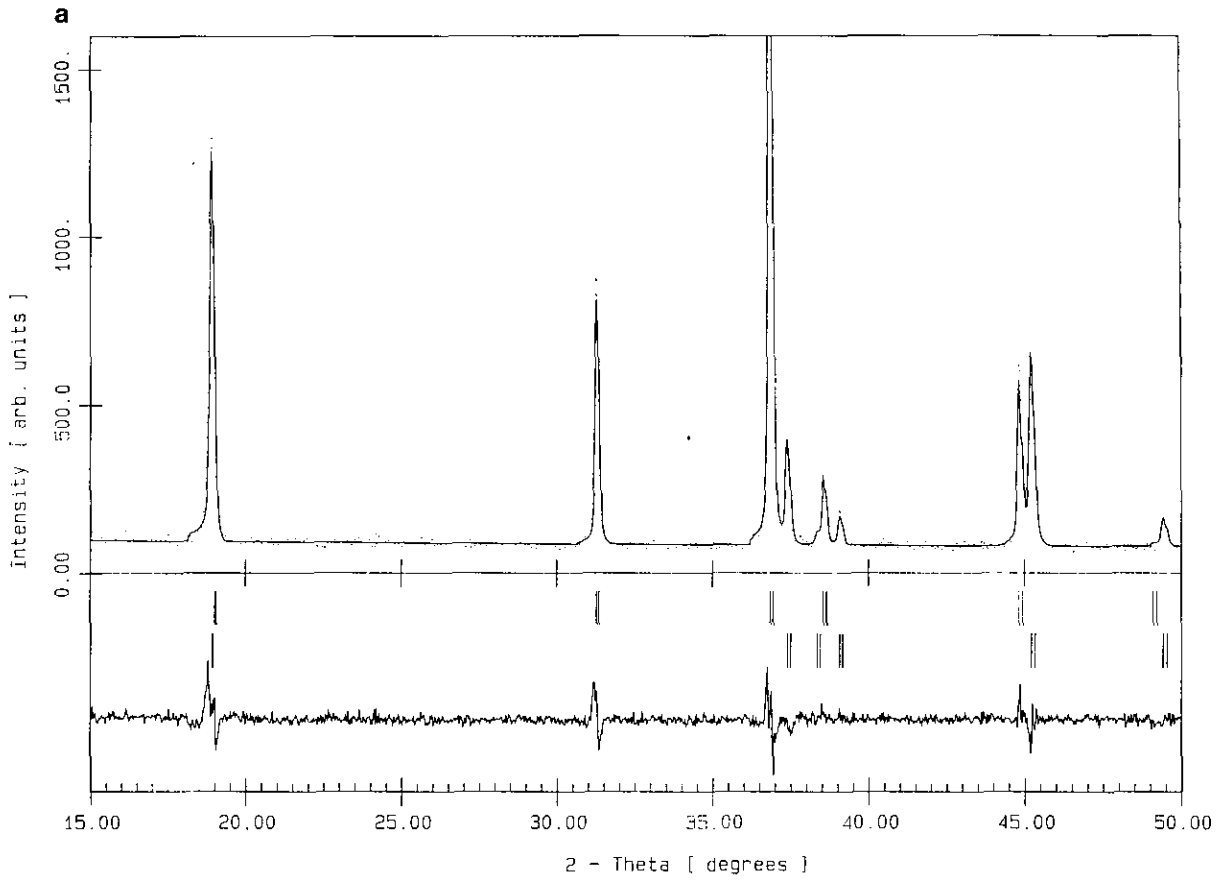

FIG. 8. Experimental (points) and calculated (continuous line) X-ray diffraction patterns of $x_{Li} = 0.20$ plaque after thermal treatment at 800°C: (a) angular range 15°–50° (2θ); (b) angular range 50°–85° (2θ). Below the patterns: peak positions of the phases (bars); difference between experimental and calculated (continuous line).

mass, rather than to mass change, it is easy to show that the final mass expected on the basis of X-ray data is only 0.66% lower than the measured one, indicating that there is a substantial agreement between the two types of data. Thus it is seen that the main consequence of the increase in the temperature of the thermal treatment from 800 to 1300°C is the appearance of a consistent amount of stoichiometric CoO together with stoichiometric Co_3O_4. It was previously noted that the only oxide present at temperatures higher than about 930°C is CoO and that, provided the cooling rate is low enough (as in the present work), it completely transforms into Co_3O_4 during sample cooling (see the values for mass change (Table 1) and phase composition (Table 2) of pure Co mixtures treated at 1100°C for a confirmation). However, if considerable sinterization takes place as a consequence of a high temperature thermal treatment, it is possible that during cooling oxygen cannot reach the bulk of the grains with the result that part of the CoO fails to transform into Co_3O_4. Such a hypothesis is confirmed by SEM micrographs which show that grain growth becomes appreciable at 1200°C (and becomes very important at 1300°C), i.e., at the temperature where the Δm values begin to decrease (Table 1) and the presence of the CoO phase is first recognized by X-ray analysis (Table 2). It can then be concluded that the presence of CoO is a direct consequence of sample sinterization.

4.4. Phase Composition and Temperature: Lithium-Containing Samples

It can be seen in Table 1 that the percentage mass changes measured after thermal treatments at 1300°C are 7.2 ($x_{Li} = 0.10$) and 9.3 ($x_{Li} = 0.20$) units lower than those recorded at 800°C. It was previously noted that lithium loss occurs for $T \geq 1100$°C. However, as the initial Li_2O content of the samples is 2.46 and 5.22% respectively, it follows that lithium oxide sublimation alone cannot explain the mass change decrease from 800 to 1300°C.

Both qualitative and quantitative information about the phase composition of the samples has been obtained by the refinement of X-ray data. The results are given in the

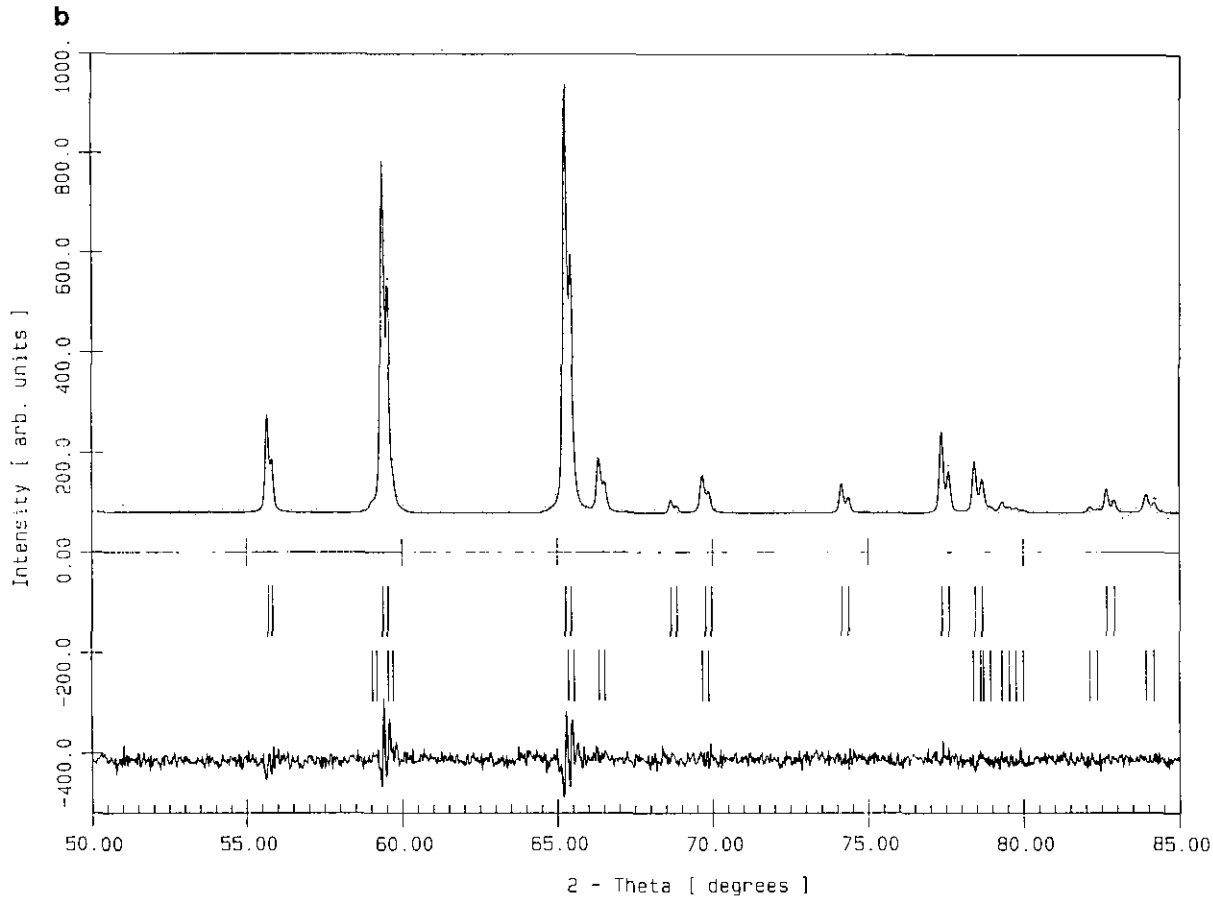

FIG. 8—*Continued*

upper part of Table 5. Once again it would be useful to compare X-ray and gravimetric results. However, the mass change data cannot be used as before to obtain the system composition because now there are at least two parameters to determine by each mass change measurement (the relative amounts of at least two phases and the stoichiometry of one of them). A reasonable way to compare the agreement between the X-ray and Δm data is to calculate the mass changes expected on the basis of the X-ray composition and stoichiometry and to compare these values with the experimental ones. The calculated percentage mass changes are given in the lower part of Table 6 while the experimental values can be found in Table 1. It can be seen that the calculated values are 1.7 (x_{Li} = 0.10) and 0.4 (x_{Li} = 0.20) units higher than the experimental ones. This means that the expected final masses agree to within 1.5% (x_{Li} = 0.10) and 0.38% (x_{Li} = 0.20) with the experimental ones and this shows that there is a substantial convergence between mass data and

TABLE 5
Phase Composition of Lithium-Containing Plaques as Deduced from X-Ray Refinement, after Thermal Treatment at 1300°C

	x_{Li}	
	0.10	0.20
X-ray	$Li_{0.036}Co_{2.964}O_{3.52}$(45.1%) CoO (54.9%)	$Li_{0.031}Co_{2.965}O_{3.70}$(28.1%) CoO (68.3%) $LiCoO_2$ (3.6%)
Calculated Δm	12.6%	4.9%

Note. The calculated Δm values represent the mass changes expected on the basis of the X-ray composition and stoichiometry.

TABLE 6
Phase Composition as Deduced from X-Ray Refinement and Mass Change Data of a Pure Co Plaque after Thermal Treatment at 1300°C

	x_{Li} = 0.00; T = 1300°C	
X-ray	Co_3O_4(63.1%)	CoO(36.9%)
Δm	Co_3O_4(72.7%)	CoO(27.3%)

X-ray results. As concerns these last ones it can be noted that:

(a) the $LiCoO_2$ phase is completely absent on the $x_{Li} = 0.10$ sample while it is reduced to a very low mass percentage in $x_{Li} = 0.20$ sample;

(b) the Co_3O_4 phase is still highly nonstoichiometric but different from before a small amount of lithium substitutes for Co into the cationic sublattice of Co_3O_4;

(c) consistent amounts of CoO are present in both samples. However, the mixture richer in lithium has the higher CoO content and both lithium-containing samples have CoO mass fractions considerably higher than that shown by a pure Co sample after the same thermal treatment (see Table 6).

Point (a) is due to $LiCoO_2$ decomposition, as confirmed by a TGA analysis performed on a pure, commercial $LiCoO_2$ sample. Point (b) indicates that the nonstoichiometry of Co_3O_4 does not depend appreciably on the temperature of the thermal treatment but rather on the presence of lithium carbonate in the starting mixture. This follows from the fact that lithium-containing samples show nonstoichiometric Co_3O_4 while pure Co samples have stoichiometric Co_3O_4 independent of the temperature of the thermal treatment. Regarding point (c), the presence of CoO can be explained by the same arguments previously used for pure Co samples. Moreover, the fact that the relative amount of CoO increases with increasing Li_2CO_3 content of the starting mixture suggests that an increased lithium content of the samples makes the sinterization easier.

4.5. Lithium Content, Sinterization, and Microstructure

SEM micrographs support and complete the conclusion reached thus far on the positive role that the presence of Li_2CO_3 in the starting mixture exerts on sample sinterization. It can be seen in Figs. 5a, 6a, and 7a that the mean particle size is nearly the same at 800°C on both lithiated and pure Co samples. Li_2CO_3 is completely decomposed at this temperature and the entire lithium content of the sample is in the form of $LiCoO_2$. This means that neither Li_2CO_3 itself, nor the formation of $LiCoO_2$ exert any direct and appreciable effect on sample particle size. However, at 1000 and 1100°C the mean particle size is considerably higher on lithiated than on pure Co samples (Figs. 5b, 5c, 6b, 6c, 7b, and 7c) indicating that sinterization starts at lower temperatures on the first ones. An appreciable grain growth due to sinterization takes place only at 1200 and 1300°C on pure Co samples (Figs. 5d and 5e). However, at such high temperatures, $LiCoO_2$ decomposition and consequent Li_2O sublimation occur on lithium-containing samples. Both processes oppose grain growth and the result is that the mean particle size of the lithiated and pure Co samples again becomes comparable at 1200 and 1300°C (Figs. 5d, 5e, 6d, 6e, 7d, and 7e).

The picture deduced from SEM micrographs is confirmed and completed by ΔPDC, porosity, and density measurements. The ΔPDC data (Fig. 4) are consistent with an increasing difference in the grain growth rate of pure Co and lithiated samples in the temperature range 800–1100°C and with a decrease in such a difference at higher temperatures. Also expected on the basis of SEM micrographs is the fact that Hg porosity is nearly the same for pure Co and lithiated samples at both 800 and 1200°C (Table 3). However, total porosity ($T = 800$°C) is higher on lithiated than on pure Co samples due to the higher contribution of microporosity in the former. It is likely that CO_2 evolution (from Li_2CO_3 decomposition) during Co oxidation plays a part in the higher microporosity of lithiated samples.

5. SUMMARY AND CONCLUSIONS

It was shown by X-ray and gravimetric measurements that a highly nonstoichiometric Co_3O_4 forms in lithium-containing samples while a stoichiometric oxide is always obtained from pure Co samples subjected to the same thermal treatment. It was also shown that sinterization plays an important role in sample phase composition and is responsible for the relative amount of CoO present at room temperature in the reacted mixture. It was argued from the quoted measurements and confirmed by SEM and ΔPDC measurements that lithiated samples show a higher sinterization rate than pure Co ones at "low" temperatures ($T \leq 1100$°C) and that the sinterization rates become quite similar at high temperatures. It is very likely that the increased sinterization rate of lithium-containing mixtures is due to the highly defective structure of the Co_3O_4 obtained from them. On the other hand, at $T \geq 1100$°C $LiCoO_2$ decomposition and Li_2O sublimation occur and, as previously seen, this decreases the sinterization rate of lithiated samples. The fact that sinterization can be appreciably affected by the amount of Li_2CO_3 in the starting mixture could be used to exert some degree of microstructural control of the products. As an example, it is shown in Table 3 that microstructural parameters are quite different for $x_{Li} = 0.00$ and $x_{Li} = 0.10$ samples. However, this is an argument of preeminent technological interest and is not developed in detail in this paper.

It has to be noted as a final remark that after all both the nature and the relative amount of the final products are strongly affected by the stoichiometry of the first oxide (Co_3O_4) formed during the reaction. It might then be asked why a nonstoichiometric Co_3O_4 is obtained when cobalt oxidation occurs in the presence of lithium carbon-

ate. The reason, at present, is not completely clear. However, it is likely that some crystallographic reason is involved in the phenomenon. This is suggested by the fact that the CoO obtained after thermal treatments at high temperatures shows a strong preferred orientation on lithium-containing samples but not on pure Co ones. Moreover, as previously noted, the CoO reflections obtained on lithiated samples are slightly shifted toward higher angles than those of pure Co ones, confirming that there is some crystallographic difference between the CoO obtained from lithiated and pure Co samples.

REFERENCES

1. N. Q. Minh, *J. Power Sources* **24,** 1 (1988).
2. G. H. Kucera, J. L. Smith, and A. P. Brown, *Proc. Electrochem. Soc.* **14,** 137 (1989).
3. L. Plomp, E. F. Sitters, C. Vessies, and F. C. Eckes, *J. Electrochem. Soc.* **138,** 629 (1991).
4. J. B. J. Veldhuis, F. C. Eckes, and L. Plomp, *J. Electrochem. Soc.* **139,** L6 (1992).
5. L. Plomp, J. B. J. Veldhuis, E. F. Sitters, and S. B. van der Molen, *J. Power Sources* **39,** 369 (1992).
6. A. Pigeaud, H. C. Maru, L. Paetsch, J. Doyon, and R. Bernard, *in* "Proceedings, Symp. Porous Electrodes: Theory and Practice, (H. C. Maru, T. Katan, and M. G. Klein, Eds.), Electrochem. Soc., Pennington, NJ, 1984.
7. E. Antolini, M. Leonini, V. Massarotti, A. Marini, V. Berbenni, and D. Capsoni, *Solid State Ionics* **39,** 251 (1990).
8. E. Antolini, A. Marini, V. Berbenni, V. Massarotti, D. Capsoni, and R. Riccardi, *Solid State Ionics* **57,** 217 (1992).
9. H. M. Rietveld, *J. Appl. Crystallogr.* **2,** 65 (1969).
10. D. B. Wiles and R. A. Young, *J. Appl. Crystallogr.* **14,** 149 (1981).
11. V. Massarotti, D. Capsoni, V. Berbenni, R. Riccardi, A. Marini and E. Antolini, *Z. Naturforsch A* **46,** 503 (1991).
12. W. A. Dollase, *J. Appl. Crystallogr.* **19,** 267 (1986).
13. R. J. Hill and C. J. Howard, *J. Appl. Crystallogr.* **20,** 467 (1987).
14. Natl. Bur. Stand. (U.S.), Circ. 539, 9 29, (1960); JCPDS Card N.9-418.
15. Johnston, R. R. Heikes, and D. Sestrich, *J. Phys. Chem. Solids* **7,** 1 (1958); JCPDS Card N.16-427.
16. W. D. Kingery, H. K. Bowen, and D. R. Uhlmann, "Introduction to Ceramics," p. 530. Wiley, New York, 1975.
17. H. P. Klug and L. E. Alexander, "X-Ray Diffraction Procedures," 2nd ed., Chap. 7. Wiley, New York, 1974.
18. G. W. Brindley, *Philos. Mag.* **36,** 347 (1945).
19. P. M. de Wolff, *Physica* **13,** 62 (1947).
20. Z. W. Wilchinsky, *Acta Crystallogr.* **4,** 1 (1951).
21. M. Shimazu, *Mineral J.* **5,** 180 (1967).